Supporting Information

Sagiyama et al. 10.1073/pnas.1323855111

SI Materials and Methods

Animal Protocol. The animal protocols were approved by the institutional animal care and use committee, and the experiments were performed in accordance with the National Institutes of Health Guidelines on the Use of Laboratory Animals. The human orthotopic tumor mouse model of glioblastoma multiformes (GBMs) developed by Bachoo et al. were exploited (1, 2). Within 2–3 h of surgical resection of the glioblastoma from a human patient, 5×10^4 viable tumor cells were injected stereotactically into the caudate region of nonobese diabetic SCID mouse brains. The mice were killed when they had developed focal neurological deficits, intractable seizures, or significant weight loss (>20%). When mice were moribund, the tumor cells were harvested, and their fragments were saved for genomic, protein, histopathological, and biochemical analysis. At the same time, a section of the tumor was gently dissociated and reinjected intracranially into new nonobese diabetic SCID mice. This process has been serially repeated for maintaining as the orthotopic tumor lines in vivo.

MRI. MRI was conducted with a 7-T small-animal MR system (Varian) with a 40-mm (i.d.) radiofrequency coil. All animals were anesthetized with 1–2% isoflurane (Aerrane; Baxter) mixed in 100% oxygen. They were placed head-first in the supine position in the system with a respiratory sensor and with the head centered with respect to the center of the radiofrequency coil. First, low spatial resolution localizer imaging was performed to confirm reproducible positioning. High-resolution axial T2-weighted (T2W)/T1-weighted (T1W) images were obtained to cover the entire brain with a fast spin-echo sequence (repetition time/echo time, 500/10.3 ms for T1W imaging, 2,500/60 ms for T2W imaging; field of view, 25.6 × 25.6 mm; matrix, 256 × 256; slice thickness, 1 mm; gapless; number of excitations, 4). On a single 1-mm-slice delineating the tumor, amide proton transfer (APT) imaging was performed. Gradient-echo images were obtained following a presaturation pulse (continuous-wave block pulse; B1, 2.3 μT; duration, 5 s), which was applied at 29 frequency offsets from 7 to −7 ppm with an interval of 0.5 ppm. Other imaging parameters were: repetition time/echo time, 6.52/3.16 ms; flip angle, 20°; field of view, 25.6 × 25.6 mm; matrix, 128 × 64 (reconstructed to 256 × 256); and number of excitations, 8. A control image with the saturation offset at 300 ppm was also acquired. Total acquisition time for each animal was ∼50 min.

Histological Examination. Four mice from each group in experiment I and three mice from each group in experiment II were killed, and brains were harvested after the final MRI session for histological analysis. Pathologic slices were obtained in an axial plane corresponding to MR images and stained with H&E, Ki67, and caspase-3 immunohistochemical staining for microscopic examination. The primary antibodies and their dilutions were as follows: monoclonal antibody to Ki67/MIB-1 (prediluted; no. 790–4286; Ventana Medical Systems) and poly/monoclonal antibody to caspase-3 (1:200; no. 9661; Cell Signaling). All immunostains were performed on the Benchmark XT stainer using CC1 pretreatment solution (95 °C for 30 min) and the XT UltraView Universal DAB detection system (Ventana Medical Systems). Three fields with magnifications of 20× (0.12 mm^2 per field) were selected at different locations evenly inside each tumor, and the total number of tumor cells and number of positive cells in Ki67 and caspase-3 staining were manually counted in each field. The percentage of cells that showed positive on Ki67 staining [Ki67 labeling index (Ki67LI)] and caspase-3 staining were calculated for recognition of proliferation and apoptosis, respectively. The cell density, Ki67LI, and apoptosis rate in the three fields were averaged for a representative value for each animal.

Total protein was measured by using standard published protocols (3) in tumors from control and treated animals. Briefly, the tumor tissue was homogenized and all water-soluble protein was extracted into RIPA buffer (no. 89900; Thermo Scientific) before total protein was measured by Bradford assays (no. 500-001; Bio-Rad).

Statistical Analysis. All values are expressed as mean ± SD. Interobserver agreement for the corrected APT ratio (APTR) of tumor from the two readers was analyzed by calculating the intraclass correlation coefficient and a simple linear regression analysis. Intraclass correlation coefficients are considered to be excellent if greater than 0.75 (4). Because the measured corrected APTR by the two observers agreed well, they were averaged in each animal for further analysis. The Student *t* test was used to compare between the two groups in following parameters; tumor volume, percentage change of tumor volume, percentage change of enhanced area on APT weighted (APTW) image, percentage change of corrected APTR, cell density, apoptosis rate, Ki67LI, and total amount of protein in tumors. Temporal changes of area on APTW image and corrected APTR between baseline and 1 wk in each group were analyzed by paired *t* test. The association between the corrected APTR and tumor volume or Ki67LI was evaluated with a simple linear regression analysis. All statistical analyses were performed by using commercially available software (Prism 5.0; GraphPad), and $P < 0.05$ was considered to indicate a statistically significant difference.

1. Marian CO, et al. (2010) The telomerase antagonist, imetelstat, efficiently targets glioblastoma tumor-initiating cells leading to decreased proliferation and tumor growth. *Clin Cancer Res* 16(1):154–163.
2. Marin-Valencia I, et al. (2012) Glucose metabolism via the pentose phosphate pathway, glycolysis and Krebs cycle in an orthotopic mouse model of human brain tumors. *NMR Biomed* 25(10):1177–1186.
3. Sambrook J, Fritsch EF, Maniatis T (1989) *Molecular Cloning: A Laboratory Manual* (Cold Spring Harbor Lab Press, Cold Spring Harbor, NY) 2nd Ed.
4. Shrout PE, Fleiss JL (1979) Intraclass correlations: Uses in assessing rater reliability. *Psychol Bull* 86(2):420–428.

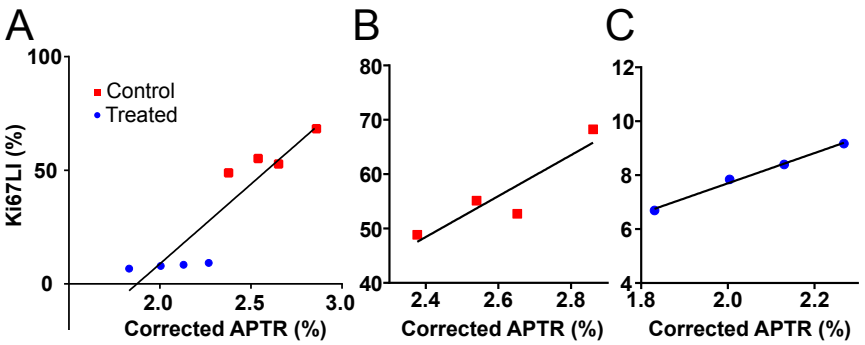

Fig. S1. Correlation between the corrected APTR and the Ki67LI (i.e., percent of cells that are Ki67-positive). (*A*) The Ki67LI showed a positive correlation with the corrected APTR ($P < 0.01$; $r^2 = 0.84$). Although this correlation tended to also be shown in each group (*B* and *C*), the result was not conclusive because of the limited number of sample ($n = 4$ per group).

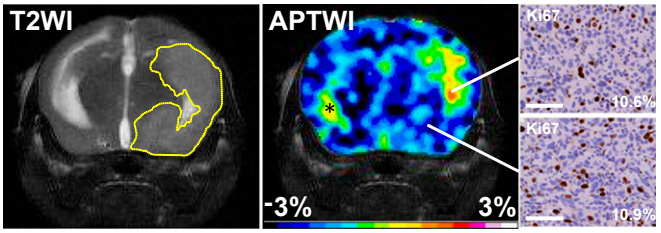

Fig. S2. Regional comparison of Ki67 staining between the region with and without enhancement on APTW image in the treated tumor. The tumor was still observed (dotted line) on T2W image (*Left*). The enhancement area (green to red on APTW image; *Middle*) that was seen in entire tumor before the treatment was reduced and remained in a part of the GBMs. Concurrently, Ki67 staining was homogenously reduced throughout the tumor, and there were no differences between the regions showing enhancement (*Upper Right*) and no enhancement (*Lower Right*) on the APT imaging. The numbers in the right bottom corner are Ki67LI values in the regions. (Scale bars: 100 μm.) Area marked with an asterisk on the APTW image is the expanded ventricle.